Research Journal of Applied Sciences, Engineering and Technology 6(2): 316-319, 2013
ISSN: 2040-7459; e-ISSN: 2040-7467

Submitted: October 31, 2012 Accepted: December 22, 2012 Published: June 10, 2013

Effect of Reservoir Velocity on AVO Intercept-Gradient Crossplot

[1]Chen Xiao-Hong,[1]Liu Zhan, [2]Chen Xiao-Cheng and [3]Wang Yun-Zhuan
[1]School of Geosciences, China University of Petroleum, Qingdao 266580, China
[2]Shengli College, China University of Petroleum, Dongying 257061, China
[3]Northeast Petroleum University, Daqing 163318, China

Abstract: Richer Amplitude Versus Offset (AVO) attributes information can be extracted with the continuous improvement of the AVO crossplot and the advancement of superimposed inversion technology. The variation of reservoir thickness and Poisson's ratio is analyzed intuitively on the crossplot combined with the oil and gas physical meaning of the two attributes and their relationship. The anomalies of oil and gas or lithology are identified and explained according to some priori information. In this study, based on the Shuey approximate formulas simplified from the full form of the Zoeppritz equation, the models' angle gathers are extracted and the P-G crossplot of AVO has been drawn. The effect of reservoir velocity on the AVO crossplot are compared and analyzed. Results find the parameters selected in this research are appropriate and the rules are obvious. Analyzing the effect of reservoir velocity on the AVO intercept-gradient crossplot is helpful to the exploration of natural and light oil in regions with a priori information.

Keywords: AVO, crossplot, gradient, intercept, reservoir velocity

INTRODUCTION

Reasonably explaining the AVO anomaly is the core problem of AVO study because not all anomalies are caused by the presence of oil and gas, in particular cases they may be caused by the lithology change and noise. AVO crossplot is a widely used important technology to explain and analyze AVO attributes. The main idea of AVO crossplot is to project the AVO attributes onto the crossplot plane first, so the data corresponds to different lithology and containing fluid composition will be distributed in different regions of the crossplot plane and then intuitively analyze the variation of two crossed AVO attribute factors combined with their oil and gas physical meaning and the relationship between them, finally, identify and explain the oil and gas or lithological anomaly according to some priori information (Zhang *et al*., 2002; Wang, 2003; Cheng and Zhang, 2003; Sun *et al*., 2004; Ma and Morozov, 2010; Aaron *et al*., 2007).

With the continuous improvement and development of AVO crossplot and the progress of the superposition inversion technique, richer AVO attribute information can be extracted and chosen to analyze the crossplot, such as the intercept-gradient, near trace stack-far trace stack, transverse wave impedance-longitudinal wave impedance, (Wang *et al*., 2005; Avseth *et al*., 2008; He *et al*., 2001). Comprehensively utilizing these attributes to analyze the crossplot can improve the analysis and explain reliability of AVO. However, the priori information of well data is needed to ensure the analysis reasonability of crossplot with many attributes (such as longitudinal wave velocity-Poisson's ratio), therefore, the application of certain attributes crossplot is limited in areas without available well data (He *et al*., 2005; Christopher, 2000; Wang *et al*., 2003).

At present, there are many AVO attributes crossplot in which the intercept-gradient crossplot can obtain a good analysis effect even in areas without available well data. The intercept-gradient crossplot has been widely studied for many years by scholars in the world(Tim *et al*., 2001). Smith and Gidlow pointed out that the crossplot with the AVO intercept and gradient extracted from earthquake can often form a "background trend" with clear meaning and the offset of this trend can be used as the showing of oil and gas (Smith and Gidlow, 1987). The analysis and explain technologies of such crossplot are relative mature, rather few effect of the reservoir velocity has been studied. In this study, the Widess graphic formula is taken as a guide and the effect of reservoir velocity on the P-G crossplot has been determined.

FUNDAMENTAL OF AVO

Zoeppritz equation used mostly to describe the reflection and transmission of plane wave is chosen to form the theoretical basis of the AVO technique (Lu, 1993). The full form of equations is difficult to be

Corresponding Author: Chen Xiao-Hong, School of Geosciences,China University of Petroleum, Qingdao, Shandong 266580, China, Tel.: 15953287462

applied directly for its mathematical complexity and physical non-intuitivity. Shuey (1985) analyzed the effect of Poisson's ratio on the reflection coefficient based on the previous study (Akiand Richards, 1980) and simplified the Zoeppritz equation, the given simplified formula is the Zoeppritz approximate equation (Castagna *et al*., 1998) used mostly at present.

Shuey (1985) proposed that it is much more complicated to study the problems involved in absolute amplitude than relative amplitudes and given the relative reflection coefficient equation follows:

$$R(\alpha)/R_0 \approx 1 + A\sin^2\alpha + B\left(\tan^2\alpha - \sin^2\alpha\right) \quad (1)$$

where,

$$R_0 \approx \frac{1}{2}\left(\frac{\Delta v_P}{v_P} + \frac{\Delta\rho}{\rho}\right)$$

$$A = A_0 + \frac{1}{(1-\sigma)^2}\cdot\frac{\Delta\sigma}{R_0}$$

$$A_0 = B - 2(1-B)\frac{1-2\sigma}{1-\sigma}$$

$$B = \frac{\Delta v_P / v_P}{\Delta v_P / v_P + \Delta\rho/\rho}$$

$$\Delta\sigma = \sigma_1 - \sigma_2$$

Equation (1) shows that the combined effect of the elastic properties at both sides of the elastic interface media is valid when incidence angle changes continuously within a certain range. The function $\tan^2\alpha$-$\sin^2\alpha$ approaches zero when the incident angle is in the range of 0°-30° namely, the third term has almost no effect on the reflection coefficient. But the third term plays a leading role to the reflection coefficient when the incident angle is greater than 30°.

Multiply Eq. (1) by R_0, the Zoeppritz approximate equation can be expressed with the absolute amplitude:

$$R(\alpha) \approx R_0 + \left[A_0 B_0 + \frac{\Delta\sigma}{(1-\sigma)^2}\right]\sin^2\alpha + \frac{1}{2}\frac{\Delta v_P}{v_P}\left(\tan^2\alpha - \sin^2\alpha\right) \quad (2)$$

Equation (2) is the simplified formula to highlight Poisson's ratio, the relationship between Poisson's ratio and the absolute amplitude can be clearly seen from this equation. The formula above can be simplified as follows in practical application:

$$R_{PP}(\alpha) = A + B\sin^2\alpha + C\left(\tan^2\alpha - \sin^2\alpha\right) \quad (3)$$

where the third term can be ignored for it is very small when the incidence angle α is less than 30°, then the Eq. (3) can be simplified as:

$$R_{PP}(\alpha) = A + B\sin^2\alpha \quad (4)$$

where, R_{PP} (α) is the reflection coefficient of P-wave, A and B what are called intercept P and gradient G can be gained after fitting a straight line in the coordinate system.

MODELING ANALYSIS OF AVO CROSSPLOT

The reservoir parameter chose in this study is the velocity, the single-interface model with two-layer medium and two-interface model with three-layer medium are designed to study the variations of it. The upper part of the single-interface model is the surrounding rock formation, the lower one is the reservoir, generally sandstone. Among the double-interface model is the sandstone reservoir and the upper layer and lower layer of it are the surrounding rock with the same lithology. The Ricker wavelet with the frequency of 50 Hz is chosen to composite the angle gathers and finally the contrast analysis is completed after producing the P-G crossplot in the EXCEL.

Single-interface model: Figure 1 shows the two-layer medium in single-interface model, the velocity of longitudinal wave in the upper formation I is 2500 m/s, where the Poisson's ratio is 0.4, the density ρ1 is 2.0 g/cm^3. The Poisson's ratio is 0.1, density is 1.8 g/cm^3 and the velocityoflongitudinalwave changes with a different value in the lower reservoir II. The effect of velocity on AVO characteristics has been studied by changing the longitudinal wave velocity of lower reservoir which is defined as 2600, 2700, 2800, 2900 and 3000 m/s, respectively.

Figure 2 shows all the trend lines pass through the origin and the trend lines rotate counterclockwise as the

I $V_{p1} = 2500\text{m/s},\ \sigma_1 = 0.4,\ \rho_1 = 2.0\text{g/cm}^3$

II $V_{p2},\ \sigma_2 = 0.1,\ \rho_2 = 1.8\text{g/cm}^3$

Fig. 1: Single-interface model with two-layer formation medium

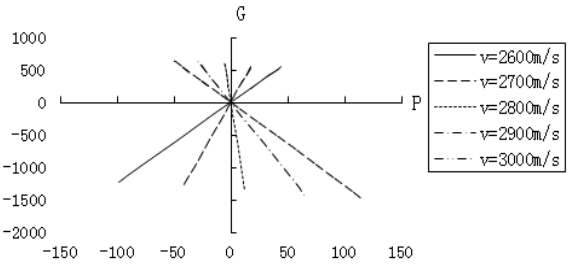

Fig. 2: P-G crossplot of single-interface model when the poisson's ratio is 0.1

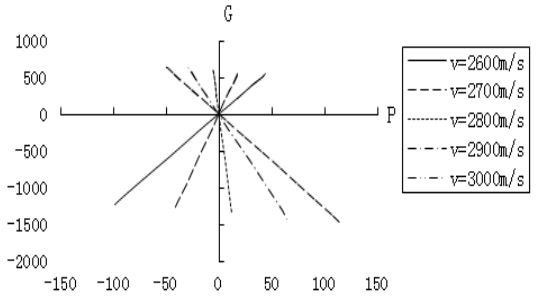

Fig. 3: P-G crossplot of single-interface model when the poisson's ratio is 0.4

I	$V_{p1} = 2500\text{m/s}, \sigma 1 = 0.4, \rho_1 = 2.0\text{g/cm}^3$
II	$V_{p2}, \sigma 2 = 0.1, \rho_1 = 1.8\text{g/cm}^3$
III	$V_{p1} = 2500\text{m/s}, \sigma 1 = 0.4, \rho_1 = 2.0\text{g/cm}^3$

Fig. 4: Double-interface model with three-layer formation medium

reservoir velocity increases when the Poisson's ratio in the single-interface model is 0.1. The wave impedance in lower layer changes greater than it in upper layer gradually. The slope of trend lines change from positive to negative. The slope is positive when the difference of wave impedance between lower layer and upper layer is negative while the slope is negative when the difference is positive. The angle between the trend line and P-axis increases as the increase of the difference of wave impedance. G values remain the same and P values change.

Figure 3 shows all the trend lines rotate clockwise as the reservoir velocity increases when the Poisson's ratio in the single-interface model is 0.4. The wave impedance in lower layer changes greater than it in upper layer gradually. The slope of trend lines change from negative to positive. The slope is negative when the difference of wave impedance between lower layer and upper layer is negative while the slope is positive when the difference is positive. The angle between the trend line and P-axis increases as the increase of the difference of wave impedance. G values remain the same and P values change.

Double-interface model: Figure 4 shows the three-layer medium in double-interface model, the velocity of longitudinalwave in the upper formation I is 2500 m/s, where the Poisson's ratio is 0.4, the density ρ1 is 2.0 g/cm^3. The Poisson's ratio is 0.1, density is 1.8 g/cm^3, thickness is 7 m and the velocityof longitudinal wave changes with a different value in the middle reservoir II. The conditions of lowerformation III are the same as the upper formation I. The effect of velocity on AVO characteristics has been studied by changing the longitudinal wave velocity of middle II which is defined as 2600, 2700, 2800, 2900 and 3000 m/s, respectively.

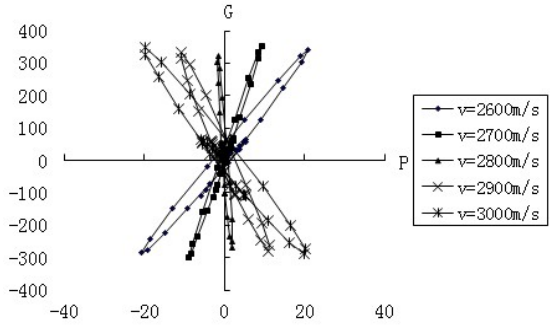

Fig. 5: P-G crossplot of double-interface model when the poisson's ratio is 0.1

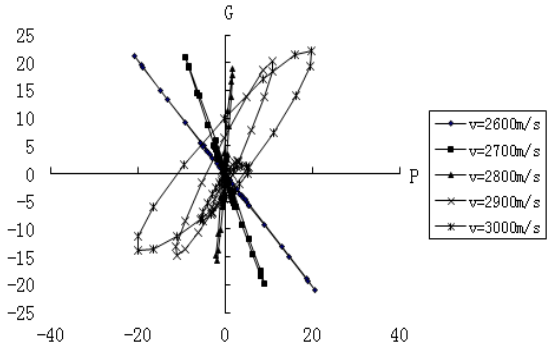

Fig. 6: P-G crossplot of double-interface model when the poisson's ratio is 0.4

As is shown in Fig. 5, the fitting point is no longer a relationship of straight line but an approximate ellipse when the Poisson's ratio in the double-interface model is 0.1. The "major axises" of these ellipses rotate counterclockwise as the reservoir velocity increases. The wave impedance in lower layer changes greater than it in upper layer gradually. The slope of major axis of the ellipse changes from positive to negative. The slope is positive when the difference of wave impedance between lower layer and upper layer is negative while the slope is negative when the difference is positive. The angle between the major axis and P-axis increases as the increase of the difference of wave impedance. Just like the single interface model, G values remain the same and P values change. The intercept in the G-axis first decreases and then increases.

As is shown in Fig. 6, the "major axises" of these ellipses rotate clockwise as the reservoir velocity increases when the Poisson's ratio in the double-interface model is 0.4. The intercept in the G-axis increases gradually. The wave impedance in lower layer changes greater than it in upper layer. The slope of major axis of the ellipse changes from negative to positive. The angle between the major axis and P-axis increases as the increase of the difference of wave impedance.

CONCLUSION

In the single-interface model, all the trend lines pass through the origin of P-G crossplot. The trend lines rotate counterclockwise as the reservoir velocity increases when the Poisson's ratio is small as 0.1. When the Poisson's ratio increases to the same as upper formation, the trend lines change to rotate clockwise as the reservoir velocity increases. G values remain the same and P values change.

In the double-interface model, the fitting point is no longer a relationship of straight line but an approximate ellipse. The variation trend and the distribution of curves are the same as the two-layer medium in single-interface model. The variation of intercept in the G-axis is not obvious.

The reservoir velocity directly affects the wave impedance which can be seen from the formula “wave impedance = velocity×density”, the angle between the trend line and P-axis increases as the increase of the difference of wave impedance.

The positive or negative of the difference of wave impedance between lower layer and upper layer determines the distributive quadrants of trend line. The difference of wave impedance is negative when the Poisson's ratio is 0.1 and the trend line distributes in the first and third quadrants. The difference of wave impedance is negative when the Poisson's ratio is 0.4 and the trend line distributes in the second and fourth quadrants. When there are both positive and negative difference existed, the trend lines distribute in all of the four quadrants.

Therefore, analyzing the effect of suitable reservoir parameters (reservoir velocity, *et al*) on the AVO intercept-gradient crossplot first is helpful to the exploration of natural and light oil in regions with a priori information.

ACKNOWLEDGMENT

Financial supports from the National High Technology Research and Development Program of China (Grant No: 2009AA062802).

REFERENCES

Aaron, W., E. Brian and L. Curtis, 2007. AVO as a fluid indicator: A physical modeling study. Geophysics, 72(1): C9-C17.

Aki, K.I. and P.G. Richards, l980. Quantitative Seismology: Theory and Methods. W. H. Freeman and Co., San Francisco.

Avseth, P., A. Dræge, A. Van Wijngaarden, T.A. Johansen and A. Jørstad, 2008. Shale rock physics and implications for AVO analysis: A north sea demonstration. Leading Edge, 27: 788-797.

Castagna, J.P., H.W. Swan and D.J. Foster, 1998. Frame work for AVO gradient and intercept interpretation. Geophysics, 63(3): 948-956.

Cheng, B.J. and Y.F. Zhang, 2003. The physical meaning of AVO reduced equations and its application in the oil esploration. Comput. Tech. Geophys. Geochem. Explor., 25(1): 89-93.

Christopher, P.R., 2000. Effective AVO crossplot modeling: A tutorial. Geophysics, 65(3): 700-711.

He, C., J.P. Castagna, R.L. Brown and C.B.R. Antonio, 2001. Three-parameter AVO crossplotting in anisotropic media. Geophysics, 66(5): 1359-1363.

He, C., Y.H. Cai, H. Li and F. Yang, 2005. Application of AVO attributes crossplot interpretation technique to predict carbonate reservoir. Oil Geophys. Prospect., 40(6): 711-715.

Lu, M.J., 1993. The Principle of Seismic Exploration. 1st Edn., University of Petroleum Press, Shandong, pp: 157-159.

Ma, J.F. and I. Morozov, 2010. AVO modeling of pressure-saturation effects in Weyburn CO2 sequestration. Leading Edge, 29(2): 178-183.

Shuey, R.T., 1985. A simplification of the zoeppritz equations. Geophysics, 50(4): 609-614.

Smith, G.C. and P.M. Gidlow, 1987. Weighted stacking for rock property estimation and detection of gas. Geophys. Prosp., 35(9): 993-1014.

Sun, P.Y.,J.G. Sun and X.L. Lu, 2004. Multiple attribute cross-plot analysis of PP-wave AVO. Nat. Gas Ind., 24(2): 44-47.

Tim, K., L. Skip, R. Robert and R.T. Bahal, 2001. The AVO hodogram: Using polarization to identify anomalies. Leading Edge, 20(11): 1214-1224.

Wang, Z.J., 2003. Analysis and application of AVO intersection chart. Nat. Gas Ind., 23(S1): 49-51.

Wang, W.H., Z.X. Jiang and R.F. Pan, 2003. AVO crossplot analysis and its application. J. Xi’an Petrol. Inst. Nat. Sci. Edn., 18(2): 5-9.

Wang, B.L., X.Y. Yin and F.C. Zhang, 2005. Elastic impedance inversion and its application. Prog. Geophys., 20(1): 89-92.

Zhang, W., W.X. Li and C.J. Sun, 2002. An application of AVO crossplot technique. China Offshore Oil Gas Geol., 16(4): 286-290.